Solar PV-based scalable DC microgrid for rural electrification in developing regions

Nasir, Mashood; Khan, Hassan Abbas; hussain, arif; mateen, laeeq; Zaffar, Nauman Ahmad

Published in:
IEEE Transactions on Sustainable Energy

DOI (link to publication from Publisher):
10.1109/TSTE.2017.2736160

Publication date:
2018

Solar PV Based Scalable DC Microgrid for Rural Electrification in Developing Regions

M. Nasir, H. Khan, A. Hussain, L. Mateen and N. Zaffar

Abstract **—In this paper we present the planning, design, analysis and implementation of a highly distributed solar PV based off-grid DC microgrid architecture suitable for rural electrification in many developing countries. The proposed architecture is superior in comparison to existing architectures for rural electrification due to its a) generation and storage scalability b) higher distribution efficiency (due to distributed generation and distributed storage for lower line losses) and c) ability to provide power for larger communal loads by incorporating usage diversity without the requirement for a large dedicated generation. The proposed microgrid architecture consists of several nanogrids (households) that are capable of self-sustained generation, storage and bidirectional flow of power with the microgrid. The bidirectional power flow capability and distributed voltage droop control is implemented through the duty cycle control of a modified flyback converter. Detailed analysis on power flows, losses and system efficiencies have been conducted through Newton-Raphson method modified for DC power flow at different distribution voltage levels, conductor sizes and schemes of interconnection between contributing nanogrids. A scaled down version of the proposed architecture with various power sharing scenarios is also implemented on hardware with satisfactory results.**

Index Terms**-- Distributed Generation, Newton-Raphson Method, Rural-Electrification, Microgrid**

I. INTRODUCTION

Our current power systems are largely based on constraints of distribution systems established over a century ago. AC power systems allowed efficient transformation of voltages from one level to another, allowing power to be carried long distances with minimum line losses [1]. This fact made the AC power networks the main choice for power transmission and distribution. However, limited funds to construct new large power plants and high cost of long distance transmission lines (over 1 million USD/km [2]) are some of the constraints in meeting the growing energy demands especially for non-electrified regions.

According to the International Energy Agency (IEA), 1.3 billion people living in developing countries, i.e. ~20% of world population is without access to reliable electricity [3]. Resource constraints of developing countries hinder taking on mega projects to produce and supply energy to these communities in a reliable manner. Alternatively, various standalone solar photovoltaic (PV) systems have been incorporated as a stop-gap measure to provide rural occupants with basic electricity [4, 5]. These systems have provisions to provide few watts to few tens of watts for a rural house. However, these individual standalone solutions are suboptimal as without resource sharing they do not take advantage of usage diversity. The need is to provide these rural regions with ample electricity for basic electrification along with provision of higher powers for communal loads such as school, basic health units and water pumping and filtration plants.

Fortunately, most of the regions in South-East Asia and Africa have abundance of sunlight (above5.5 kWhr/m^2/day for most regions) [6, 7]. This makes solar photovoltaic (PV) generation an attractive alternative to conventional electricity generation. Compared to traditional AC distribution, DC microgrids are significantly more efficient due to no DC-AC or AC-DC conversion when implemented with DC distributed generation (DG). These systems have end-to-end efficiency of around 80% (for DC loads) compared to AC microgrids which are less than 60% efficient [8-10]. Therefore, the focus here is LVDC where costly up-conversions (to kV range) and the subsequent down-conversions are not required due to shorter distribution distances at a village level. Diminishing costs of solar PV panels coupled with high solar insolation, maturing of battery industry and influx of robust power electronic devices makes solar PV highly suitable for distributed electricity production.

II. RELATED WORK

Solar PV based rural electrification architectures for DC microgrids that have been presented in literature use

1. Centrally located generation (referred as central generation) with centrally located battery storage (referred as central storage) [11-14].
2. Central generation with distributed storage [8, 15].

Central placement of the resources is generally beneficial from control perspective where overall generation and storage level (state-of-charge) is reliably monitored. However, it results in higher distribution losses and rigidity in terms of future expansions [16]. More critically, their field deployments at higher power loads are particularly difficult due to high capital costs required to sustain a large system with central solar generation. One stand-out approach is 'Mera Gao Power' (MGP) in India which provides only 5W of DC power to each subscribing house, with a limit of 0.2 amps; enough to power two LED lights and a mobile-phone charging point [13, 14]. The implementation involves central PV generation and central battery storage with distribution at 24V DC to subscribing houses. Although 'small power' is

Manuscript Received: xxxx accepted on xxxxxxx. This work was supported by Faculty Initiative Funding (FIF) grant from Lahore University of Management Science (LUMS).

M. Nasir is PhD candidate at Department of Electrical Engineering at LUMS, Lahore, Cantt 54792, Pakistan (e-mail: 14060018@lums.edu.pk).

H. khan and N. Zaffar are working with Department of Electrical Engineering at LUMS as assistant professor and associate professor respectively. H. khan was previously with School of Electrical Engineering, The University of Manchester, UK from 2005 to 2010 (e-mail: hassan.khan@lums.edu.pk). N. Zaffar has previously worked with Electro-Optic/Magneto-Optic Labs at University of Pennsylvania and Techlogix Pakistan Pvt. Limited (e-mail: nauman.zaffar@lums.edu.pk).

A. Hussain and L. Mateen are working as research associates with Department of Electrical Engineering at LUMS.

beautiful, it is unlikely to bring people out of poverty or contribute towards a significant uplift of a society [17]. If such a central generation central storage architecture (CGCSA) is implemented for high power household loads (50W or higher) the losses associated with the distribution of energy are significantly higher, thereby making the scheme unviable. Moreover, with the growth of population and increase in the demand of energy, such a central system is not readily scalable from generation, storage and power electronics equipment point of view for future expansions.

Another PV based ad-hoc DC migrogrid architecture for rural electrification by wardah *et al*. [18] integrates several consumers (up to 20) with single generator units. However, the overall distribution is at 48V which makes it unviable for larger household load or community load requirement. Alternatively, for higher voltage distribution at 380V, Madduri *et.al* [8, 15] presented a PV based central generation and distributed storage architecture (CGDSA). A provision of stored energy at local houses results in an increased efficiency compared to CGCSA, however, this architecture itself is still suboptimal from two aspects a) the central PV generation requires a higher upfront cost due to a large solar panel nameplate capacity required at the very outset resulting in a cost barrier and b) distribution to distant houses will cause significant system losses. Therefore, a modularly scalable architecture, efficient with respect to distribution efficiency and cost effective with respect to up-front PV panel cost is highly desirable to enable flexibility in future expansions, and provision for high power household and communal loads.

Several other contributions [19-21] present advancements in the control aspects of DC microgrids through hierarchical, supervisory and adaptive droop control schemes requiring extensive monitoring, sensing and communication which adds in terms of complexity and cost of the microgrid. From rural electrification prospective a high cost and complex system will not be viable due to upfront cost barrier.

III. CONTRIBUTIONS

Considering the limitations (a) lower distribution efficiency, (b) low power provisioning for household load, (c) absence of communal load provisioning, d) rigidity in future expansion, and e) requirements for extensive control techniques) of mentioned architectures of DC microgrid, we propose a novel solar PV based scalable, distributed generation distributed storage architecture (DGDSA) as shown in fig. 1. The proposed architecture and associated power electronic interface enables scalability along with the large scale distribution of generation and storage resources without extensive control requirements. DGDSA also enables resource sharing to extract the benefit of usage diversity and thus it can scale in power for individual homes and can also support large (kilowatt level) loads to meet the community load requirements in an efficient manner. Individual units (houses) are able to self-sustain due to local generation and storage and only the excess power is provided to the grid which results in lowering of distribution losses as line losses are associated with the excess energy only. The architecture itself has in-built advantages i.e. (a) higher efficiency due to distributed generation and distributed storage (b) Modular scalability for future expansions, (c) Efficient aggregation of power for larger loads even with limited roof-top PV (d) delivery to communal loads such as rural schools or basic health units through pooling of power from individual household units without dedicated (large) generation (e) reliable and simplified control through hysteresis based voltage droop method (enabled through localized controller without the need of central, adaptive or supervisory control and mitigates the extensive communication requirements)(elaborated in section VI)

Furthermore, the distributed nature of the proposed DGDSA makes it independently scalable in its planning as well as operation, therefore making it highly suitable for micro-economic level resource sharing. For instance, single system (panel, converter and battery) operation could start at a single house which could then grow in a scalable manner as neighbors start using a similar module. This plug-n-play capability allows lower upfront cost with high likelihood of adoption in low-income countries. *None of the other systems in architecture provide this level of scalability.*

In our earlier work, a comparative analysis of distribution efficiency among existing architectures i.e. CGCSA, CGDSA and the proposed DGDSA has been carried out using Newton Raphson method [16] modified for DC power. It has been observed that for all ranges of power provisioning, distribution voltage levels and conductor sizes, the proposed DGDSA exhibit higher efficiency, lower line losses and minimal voltage drops in comparison to the other existing schemes [16]. A summary for distribution efficiencies and voltage drops is shown in table 1.

In the current work we particularly highlight the design and planning of DGDSA which supports high power provisioning to individual household and communal load along with the scheme for the integration of power electronic interface with the distributed resources in the microgrid. Resource sharing capability along with simplified distributed droop control, which are the key enabler for scalability as well as higher power provisioning are presented with rigorous analysis of various power sharing scenarios between contributing nanogrids.

The organization of the paper is as follows: In section IV, the architecture of proposed microgrid is presented in terms of interconnection of contributing nanogrids. In section V, Newton- Raphson power flow analysis modified for the DGDSA based DC microgrid is presented. Distributed Voltage droop algorithm for the stable operation of microgrid is formulated on the basis of microgrid energy balance and is presented in section VI. Section VII presents simulation and measured results for the planning analysis and controlled operation.

TABLE I
COMPARISON BETWEEN EXISTING AND PROPOSED ARCHITECTURES

Type of Microgrid	Maximum Distribution Efficiency (%)	Worst Voltage Drops (%)	Architecture References
CGCSA	91.9	8.86	[11- 15]
CGDSA	93.4	5.33	[8, 16]
DGDSA	96.70	3.5	[17], This work

IV. Proposed Architecture of the DC Microgrid

The electrical energy architecture proposed here is a distributed type of microgrid (Fig. 1) – a small interconnected self-sustaining electrical generation, distribution and utilization system. A household is a basic building block referred as a nanogrid. A primary task is to establish an efficient mechanism via PV distributed generation (DG), to channel excess energy between connected nodes.

For instance, in fig. 2, PV panels at rooftop (home 'a') should be able to provide energy to a neighboring house (home 'b') if the PV produced power is not being utilized in home 'a' and vice versa. Similarly, if both home 'a', home 'b' up to home 'n' have surplus power then there must be a mechanism to allow this power to be utilized at communal loads. Inherently, PV panels have a potential to continuously provide power during the presence of sunlight and if not utilized properly, this power is wasted within the panel. Therefore, in a communal setting, the surplus DC power produced by all the panels must also be utilized by communal loads such as water pumping for drinking/irrigation, lighting and computing loads in school etc. Provisioning for large communal loads otherwise is often very expensive and unsustainable in rural scenarios of developing countries.

A. Model of Nanogrid

A nanogrid is a basic building block of the microgrid architecture that will integrate its resources in a scalable manner with the community (fig. 2). Each house contains a roof mounted solar panel that generates '$P^G(t)$'watts, a load which consumes '$P^L(t)$' watts at any time 't' and a battery storage whose allowable maximum and minimum limits on state-of-charge (SOC), are 'SOC_{max}' and 'SOC_{min}' respectively. The bidirectional flow of power is controlled via power electronic converters referred as central power processing unit (CPPU). CPPU contains a microcontroller, DC-DC boost maximum power point tracking (MPPT) converter and bidirectional flyback converter.

1) DC-DC Boost Converter and MPPT Controller

The output power of a PV panel is a non-linear function of temperature and incident irradiance [22]. In order to extract the maximum power out of the available solar energy '$P^{MP}(t)$' at any time 't', maximum power point tracking techniques are employed. Various schemes for MPPT under uniform and non-uniform irradiance are discussed in literature [23, 24]. In this work Perturb and observe (P&O) algorithm is employed due to its simplicity and minimum computational complexity [23]. One critical element of the converter is the DC-DC boost to the desired operational voltage of DC grid 'V^G_{rated}'. The current and voltage values are constantly being monitored by microcontroller which adjusts the duty cycle such that the desired voltage boost and MPPT is achieved for all operating conditions.

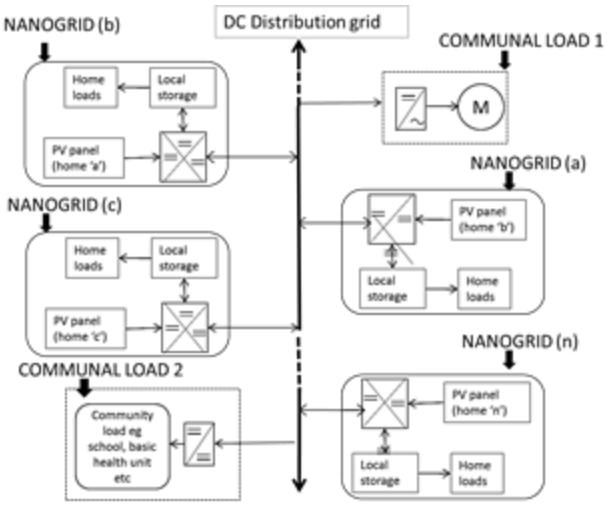

Fig. 1. Conceptual Diagram of Microgrid Architecture with Contributing Nanogrids (Households) along with Communal Loads

2) Bidirectional Flyback Converter

Bidirectional flyback converter is employed to enable resource sharing feature as it allows the transfer of power from nanogrids to microgrid or vice versa. The bidirectional power flow in the proposed flyback converter is attained through modified switch realization, i.e. replacing the diode of conventional flyback converter with another controlled mosfet switch. The switch position is also changed to ensure that the source is grounded without affecting the continuity of the circuit. This allows optimum gate driver circuit design without the requirement of complex bootstrapping circuit [25].

Flyback converter has inherent advantages of simple design and lower cost (less component usage) over other types of buck-boost converters; therefore, it is highly suitable for DC microgrid applications. Along with the higher conversion ratio, it also allows the use of inherent magnetizing inductance 'L_m' of the flyback transformer, thus mitigating the need of extra inductor for converter energy transformation. Bi-directional switch realization of flyback converter is shown in fig. 3. The continuous conduction mode (CCM) governing equation of gain 'M(d)' in terms of transformer turn ratio 'N' battery voltage '$V^B(t)$'and duty cycle 'd' of converter is

$$M(d) = \frac{V^B(t)}{V^G_{rated}} = N\frac{d(t)}{1-d(t)} \quad (1)$$

B. Model of Village and Microgrid Scheme of Interconnection

Depending upon the structure, a typical village containing 'n' houses may be segmented in 'x' segments with 'n/x' houses per segment as shown in fig. 2. The power is supplied to the load in each household via flyback converter which along with the resistance of the supplying wire is modeled as a constant power bus and is shown by distributor resistance (fig. 2).

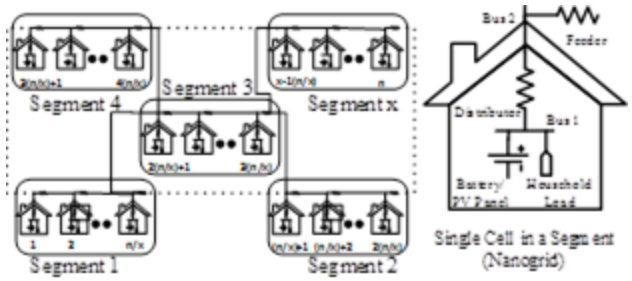

Fig.2. Proposed Architecture with Radial and Ring-Main Schemes of Interconnection

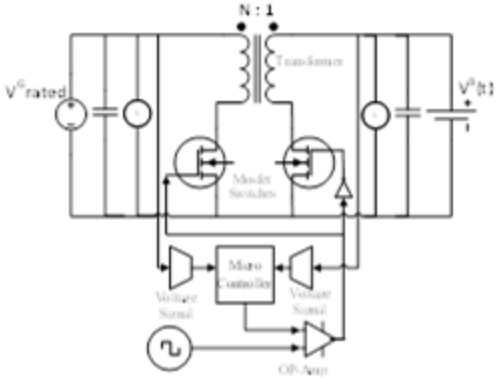

Fig. 3. Bidirectional Switch Realization and Control of Flyback Converter

The interconnection resistance between two consecutive nanogrids is modeled as feeder resistance. Two different interconnection schemes are considered and are also shown in fig. 2. The advantages of radial scheme (solid lines interconnecting various segments) include simpler design, less complexity in the laying of conductors and reduced initial cost. However uneven loading, non-uniform voltage distribution, high voltage dips at the rear end and subsequent reliability issues makes it relatively poor candidate for optimal distribution of power [26].

Therefore, in order to cope up with these issues, ring-main is proposed which connects the feeders in a ring-main fashion (dotted connection line in fig. 3), while keeping the connection of distributors intact. Thus at the cost of extra conductors high efficiency and increased reliability is achieved even at comparatively lower distribution voltages.

Using the values of feeder and distributor resistances, based upon the scheme of interconnection and topological configuration of village, a conductance matrix 'G' can be calculated for the model of the village. For a village with 'n' houses, 'G' is of the order of 2n x 2n as each house has two buses: 1) load bus at the interconnection of distributor resistance and load bus and 2) other bus at the interconnection of feeder and distributor resistance (fig. 3). Thus, elements of conductance matrix 'G_{ij}' and conductance matrix 'G' can be written in terms of individual conductance 'g_{ij}' between any two arbitrary busses i and j, where 'i' may vary from 1 to 2n.

$$G_{ij} = \begin{cases} \sum_{\substack{j=1 \\ j \neq i}}^{2n} g_{ij} & ; \forall \mathrm{i} = j \\ -g_{ij} & ; \forall \mathrm{i} \neq \mathrm{j} \end{cases} \quad (2)$$

$$G = \begin{bmatrix} G_{11} & G_{12} & \cdots\cdots & G_{1,2n} \\ G_{21} & G_{22} & \cdots\cdots & G_{2,2n} \\ \vdots & \vdots & \ddots & \vdots \\ G_{2n,1} & G_{2n,2} & \cdots\cdots & G_{2n,2n} \end{bmatrix}; G \in R^{2n \times 2n} \quad (3)$$

V. Power Flow Analysis For the Optimal Planning of Voltage Level and Conductor Size For Microgrid Operation

Power flow analysis is conducted through Newton-Raphson method and its application is modified for our DC microgrid [16]. This is essential to ascertain various critical elements of the proposed system such as total line losses, efficiency and voltage drops [27]. These parameters are used as an indicator for the selection of optimal voltage for DC microgrid. Depending upon the load requirements of each house, load is scheduled on each bus 'i' and scheduled load matrix 'P^{sch}' is

$$P^{sch} = \begin{bmatrix} P_1^{sch} & P_2^{sch} & P_3^{sch} & \cdots\cdots & P_{2n}^{sch} \end{bmatrix}^t; P^{sch} \in R^{2n \times 1} \quad (4)$$

Based upon the conductance matrix model of the village, instantaneous power at i^{th} bus 'P_i^{cal}' can be calculated as

$$P_i^{cal} = V_i I_i = \sum_{j=1}^{2n} V_i V_j G_{ij} \quad (5)$$

Therefore, calculated load matrix is 'P^{cal}' given by (6)

$$P^{cal} = \begin{bmatrix} P_1^{cal} & P_2^{cal} & P_3^{cal} & \cdots\cdots & P_{2n}^{cal} \end{bmatrix}^t; P^{cal} \in R^{2n*1} \quad (6)$$

Subtracting (4) from (6), expanding remaining terms using Taylor Series (neglecting higher order terms) [30], with $\Delta P_i^{(k)}$ = difference in Scheduled Power P_i^{sch} and P_i^{cal} for 'bus i' at k^{th} iteration and 'V^G_{rated}' is taken as reference voltage.

$$\begin{bmatrix} \Delta P_2^{(k)} \\ \vdots \\ \Delta P_{2n}^{(k)} \end{bmatrix} = \begin{bmatrix} \frac{\partial P_2^{(k)}}{\partial V_2} & \cdots & \frac{\partial P_2^{(k)}}{\partial V_{2n}} \\ : & & : \\ \frac{\partial P_{2n}^{(k)}}{\partial V_2} & \cdots & \frac{\partial P_{2n}^{(k)}}{\partial V_{2n}} \end{bmatrix} \begin{bmatrix} \Delta V_2^{(k)} \\ : \\ \Delta V_{2n}^{(k)} \end{bmatrix} \quad (7)$$

Using (7), change in voltages ΔV and corresponding bus voltage 'V_i' for 'k' iterations are found until the difference between scheduled and calculated power becomes negligible. By using the converged value of voltage at each bus, associated line losses 'LL_g', percentage line losses '$\%LL_g$', voltage drop '$\%VD_g$' and efficiency 'η_g' for the dc microgrid are calculated

$$LL_g = \frac{1}{2} \sum_{i=1}^{2n} \sum_{j=1}^{2n} G_{ij} \left(V_i \left(V_i - V_j \right) + V_j \left(V_j - V_i \right) \right) \quad (8)$$

$$\%LL_g = \frac{LL_g}{P_G} * 100\%, \text{ and } P_G = \sum_{i=1}^{n} \left(P_i > 0 \right) \quad (9)$$

$$\eta_g = 100 - \%LL_g \quad (10)$$

$$\%VD_g = \frac{V_i^{\max} - V_i^{\min}}{V_i^{\max}} * 100\% \quad (11)$$

Where, 'V_i^{max}' and 'V_i^{min}' are the maximum and minimum values of voltage at any bus after k^{th} iteration. From (6)-(11), it is apparent that line losses, efficiency and voltage drops in the microgrid system are a function of rated grid voltage 'V^G_{rated}' and conductance matrix G_{ij},.Therefore, by using the presented analysis, optimal distribution voltage and optimal conductor size may be selected for DGDSA based electrification of any village based upon number of households, power provisioning to individual household, allowable power sharing among houses and microgrid, topological configuration and scheme of interconnection.

VI. Hysteretic Voltage Droop Algorithm For Distributed Control of DGDSA

Energy balance for an ideal DGDSA based village (fig. 2) having 'n' households with distributed PV generation '$P_i^{PV}(t)$' is given by (12),based upon the constraints given in (13).

$$\sum_{i=1}^{n} P_i^{PV}(t)\Delta t = \sum_{i=1}^{n} P_i^{L}(t)\Delta t + \sum_{i=1}^{n} V_i^{B}(t)\,\Delta \mathrm{SOC}(t) \tag{12}$$

$$P^{PV}, P^{L}, V^{B}, \Delta SOC \in R^{n\times 1}$$
$$\Delta SOC_i^{\min} \le \Delta SOC_i \le \Delta SOC_i^{\min} \;;\forall t \tag{13}$$

Where, '$V_i(t)^B$' is the household battery voltage, SOC is the state-of-charge for the battery, '$SOC_i^{max}(t)$' and '$SOC_i^{min}(t)$' are allowable limits on battery SOC and '$P_i^L(t)$' is the household load power connected to battery bus drawing $I_i(t)^L$ for any time interval Δt. For the grid to be operating at rated voltage 'V^G_{rated}' with net current '$I^G(t)$' at any time t, batteries can either dump power on to the grid or take power from the grid via bidirectional flyback converter. Therefore, (12) can be written in terms of battery current '$I_i^B(t)$', which may take either positive or negative value depending upon the state of grid and subject to constraints given in (15)

$$\sum_{i=1}^{n} V^G_{rated} I_i^G(t)\Delta t = \sum_{i=1}^{n} V_i^B I_i^L(t)\Delta t + \sum_{i=1}^{n} V_i^B I_i^B(t)\Delta t \tag{14}$$

$$0 \le I_i^L \le I_i^{L,\max},\; -I_i^{B,\min} \le I_i^B \le I_i^{B,\max} \;;\forall t \tag{15}$$

Where, '$I_i^{L,max}$' is the maximum value of permissible load current at each house with '$I_i^{B,max}$' and '$I_i^{B,min}$' are the limits on battery charging and discharging current.

Based upon the duty cycle control of flyback converter, power may be channelized from microgrid to nanogrid or vice versa. If the flyback converter is operating at critical duty 'd_i^{cric}' (given by (16)), there will be zero power sharing between microgrid and battery of household 'i'. In order to set the direction and amount of power flow from microgrid to nanogrid, a positive perturb in duty 'Δd_i' is applied. Thus, flyback channelize the power from microgrid to load bus, when it is operated above critical duty '$d_i^{cric}+\Delta d_i$'. At duty below the critical duty '$d_i^{cric}-\Delta d_i$', bidirectional flyback ensures the flow of power from battery to microgrid. Thus, the stored energy in the battery may be transferred back to the grid using negative perturb in critical duty.

$$d_i^{cric}(t) = \frac{V_i^B(t)}{V_i^B(t) + NV^G_{rated}} \tag{16}$$

For stable microgrid operation duty of each flyback converter is adjusted such that it produces 'V^G_{rated}' at the microgrid side, therefore, using (1), (14) may be written as Subject to constraints given in (15)

$$\sum_{i=1}^{n} I_i^G(t) = N\sum_{i=1}^{n} \frac{d_i(t)}{\left[1-d_i(t)\right]}\left(I_i^L(t) + I_i^B(t)\right) \tag{17}$$

The stable operation of microgrid is defined by the hysteresis in grid voltage such that $V^G_{\min} \le V^G_{rated}(t) \le V^G_{\max}\;;\forall t$. Where, '$V^G_{min}$' and '$V^G_{max}$' are the minimum and maximum values of grid voltage dictated by the hysteresis that is kept generally ±2% of the rated grid voltage.

Using power balance of (17), an algorithm is formulated (shown in fig. 4) for generalized microgrid operation based upon duty cycle control of flyback converter of individual household. The Perturb in duty cycle adjusts the direction and amount of allowable power sharing between nanogrids and microgrid keeping power flows such that microgrid is always working stable region of operation.

For instance, if the grid has excess power available, the positive perturb channelize the excess power towards nanogrid battery storage or elastic load. During this situation, voltage of microgrid will decrease in proportion to the net power transfer. The formulated algorithm will ensure that if the grid voltage drops below 'V^G_{min}', the direction of power flow is reversed using a negative perturb in the duty of flyback converter to gain the balance in the voltage. Thus, a negative perturb above critical duty will channelize the stored power of the battery towards microgrid to bring its voltage above 'V^G_{min}' up to 'V^G_{max}'.

Thus, a hysteresis based voltage droop control will determine the required perturb in the duty and associated amount of power flow between microgrid and nanogrid, while keeping the voltage within hysteretic limit ensuring the stability of the scheme throughout its operation. Due to this distributed control structure, each individual nanogrid is responsible for the stable operation of microgrid. Therefore, the need of central controller and costly communication interface is omitted in the presented architecture. Further, the hysteretic based voltage droop control makes the proposed DGDSA highly scalable in terms of future expansions.

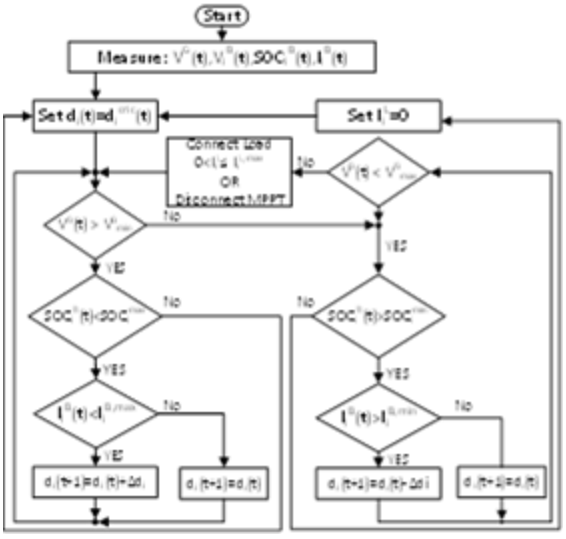

Fig.4. Hysteretic Based Distributed Voltage Droop Control

VII. Results and Discussions

For validation of the proposed methodology, a typical village of a developing country having 40 houses is considered. Each house has a PV generation capacity of 250W_P (maximum power at standard input irradiance of 1000W/m^2), 100Ah battery storage capacity and is capable of driving rated 40W of DC load including lighting, fan and charging. Village is divided in 5 segments with 8 houses per segment. The configuration of the village is considered as in fig. 2. The distance between two consecutive houses (Feeder) and internal wiring length (distributor) is taken 20m long [28].

A. Simulation Results of Power Flow Analysis for the selection of Optimal Voltage Level, Conductor Size and Scheme of Interconnection

Selection of optimum distribution voltage is a critical aspect of the microgrid as it affects the operation, control, performance, protection and safety of the microgrid based distribution systems [28, 29]. Possible levels of LVDC i.e. 48V, 120V, 230V, 325V and 400V are considered for the purpose of analysis and conductors with wire gauge areas 0.2 mm^2 (local market name 3.0-0.029"), 0.45 mm^2 (local market name 7.0-0.029"), 2.5 mm^2, 6 mm^2 and 7.5mm^2 are used for analysis. Using (2)-(11) percentage line losses, percentage voltage drop and efficiency is determined for both architectures and both schemes of interconnection to select the optimal voltage level as well as conductor size.

1) DGDSA with Radial Scheme of Interconnection

Typical and peak load scenarios are evaluated for DGDSA with radial scheme of interconnection. In typical load scenario, the power sharing between houses and grid is taken as ±20% (a house can demand 20% more or supply 20% of its rated power). Results for percentage voltage drop and efficiency (fig. 5) show that with reasonable sized conductor such as 2.5 mm^2 the distribution loss is low for 120V and higher voltages with efficiencies above 99%.

The situation changes significantly when power sharing provision is kept higher i.e. ±100%. Under this peak load scenario, a house can consume twice of its rated power and it can supply all available power to the grid. Results show that efficiency is lower for low voltages and a significantly higher cost of thick conductor must be incurred for this topology as shown in fig. 6.

2) DGDSA with Ring-Main Scheme of Interconnection

Ring main topology significantly improves the efficiencies at peak load sharing in comparison to radial topology. Ring-main interconnection topology also provides necessary redundancy to ensure service operation in grid disconnection due to a fault or broken wires. The results for peak load sharing for ring-main scheme have been shown in fig. 7. From the comparison of fig. 6 and fig. 7 it may be seen that ring-main topology for this configuration of the village has higher efficiency and less voltage drops in comparison to radial scheme of interconnection. For instance, in case of peak load sharing at 120V and 2.5mm^2 conductor size, ring-main scheme exhibits higher efficiency (95.18%) as compared to radial scheme (92.66%). In other configurations where end to end ring conductor cost is much higher as compared to respective gains in efficiencies radial scheme is the simple choice available.

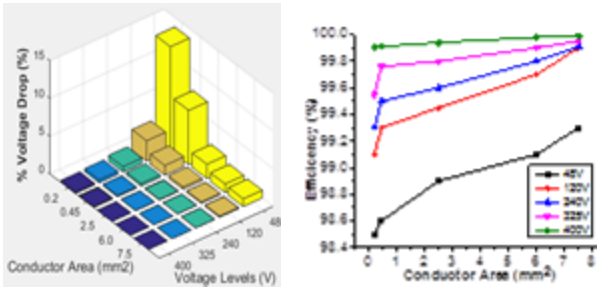

Fig. 5. Percentage Voltage Drop and Efficiency at Different Voltages and Conductor Sizes at Typical Load sharing with Radial Scheme

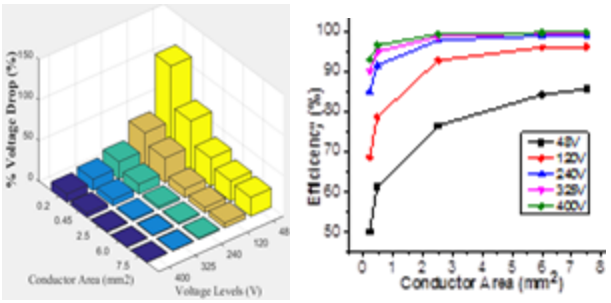

Fig. 6. Percentage Voltage Drop and Efficiency at Different Voltages and Conductor Sizes at Peak Load sharing with Radial Scheme

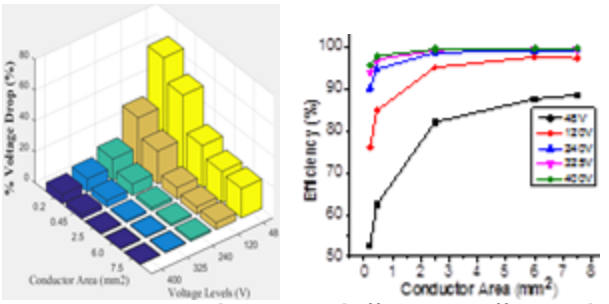

Fig. 7. Percentage Voltage Drop and Efficiency at Different Voltages and Conductor Sizes for Peak Load sharing with Ring-Main Scheme

Table. II. Shows that From 48 V to 120 V, there is a significant increase in the efficiency. The associated protection and safety requirements are not excessive [29, 30]. Moving from 120V to 400V, percentage reduction in losses is not significant, however, system complexity, protection and safety requirements increase significantly. At higher voltage levels, the system requires sophisticated and expensive protection equipment. The distributed storage and generation allows small current to flow on the grid and hazardous DC arc energy could be easily manageable even with 120V DC distribution, in comparison to 240V AC [31].

TABLE II
PEAK LOAD COMPARISON BETWEEN RADIAL AND RING-MAIN DC MICROGRID

Distribu-tion Voltage (V)	Conduc-tor Area (mm^2)	Radial Microgrid			Ring-Main Microgrid		
		LL_g (%)	VD_g (%)	η (%)	LL_g (%)	VD_g (%)	η (%)
48	2.5	23.5	34.4	76.41	17.9	27.1	82.1
120	2.5	7.34	10.9	92.66	4.82	7.38	95.18
400	2.5	0.83	1.23	99.17	0.51	0.77	99.49

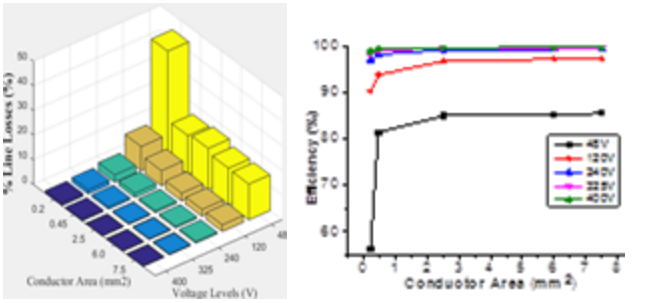

Fig. 8. Percentage Line Losses and Efficiency at Different Voltages and Different Conductor Sizes for Communal Load Case with Ring-Main Scheme of Interconnection

Moreover, voltages lower than 120V are considered safe for indirect touch and require no extra grounding and protective conductors [32]. Voltage levels lower than 48V are not suitable for distribution as voltage drop is much higher than 15%. Distribution at 120V is generally less efficient than 400V; however, ring-main interconnection between feeders largely mitigates this loss at the cost of extra conductors, and also adds necessary redundancy for a reliable operation in case of broken line or disconnection. Further analysis show, for selected parameters the losses are less than 3% even with the communal load of 400W as shown in fig. 8.

Therefore, for the considered specifications of the village, 120V with the conductor area of 2.5 mm^2 and ring main scheme of interconnection is considered optimal for microgrid interconnections. For different load specifications of other villages, proposed analysis may result in a different optimal voltage level other than 120V, based upon the trade-off between losses and cost of protection equipment.

B. Scaled Down Hardware Implementation for DC Power Flow Analysis

The proposed model that originally includes 40 houses is scaled down to four houses for practical implementation, where each house may either generate or consume the 40W of power under various scenarios. The generation capacity of each house is implemented via power supplies (ESCORT EPS3030T) and the consuming capability is implemented via DC load banks (LABTECH LEMSPL) available in the laboratory [31, 32]. Both radial and ring scenarios are tested for line losses, efficiency and voltage dips. Results are found in agreement with simulation outcomes in fig. 9.

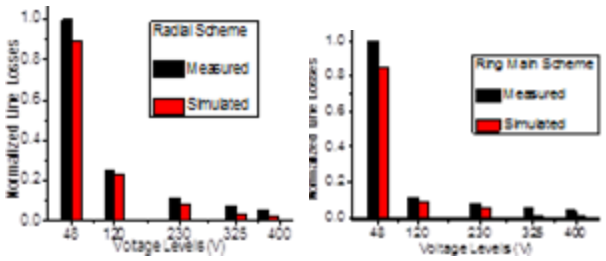

Fig. 9. Simulated v/s Measured Results for Normalized Line Losses in DGDSA with Radial and Ring-Main Schemes of Interconnection

C. Hardware Implementation of Power Electronic Interface for DGDSA based Integration of Nanogrids with Microogrid

Distribution voltage of grid 'V^{G}_{rated}' is 120V while house load distribution and storage is on 'V^{B}' 12V. Practical setup for the microgrid integration with three subatomic nanogrids is shown in fig. 10. DC microgrid is implemented using a large capacitor (5000μF) whose state of charging and discharging is being continuously monitored. For scaled down model, three houses are integrated with the microgrid such that House1 (H1) is supplying constant power and is modeled using DC power supply (ESCORT EPS3030T) [32], House2 (H2) is modeled using a 4-quadrant bipolar power supply which can act as a source or sink of power [33] and House3 (H3) consists of battery and it is tied to the grid using flyback converter.

Typical voltage variations of microgrid in various power sharing scenarios are shown region-wise in the fig. 11. In 'Region 1', House 2 and house 3 are taking power from the grid while house 1 is supplying to the grid. Based upon the algorithm presented in section V, when the power being supplied by the house 1 is not equal to the power being taken by the other two houses, the voltage of the grid will go down. Therefore, as the voltage of grid drops down below specified lower cut off 'V^{G}_{min}'=117.5V, the loads of both houses are turned off. In region 2, the power in the battery bank (house 3), house 1 and power from house 2 starts charging the grid again to take its voltage above 120 V. When the voltage is above the hysteretic threshold of the grid set as 122.5 V, the loads are turned on again as per employed algorithm. In "Region 3" House 1 and House 2 are supplying power to charge the battery of house 3. Battery voltage 'V^{B}' is also being constantly monitored during charging and discharging stage and is shown in fig. 12. The state of the system is not kept fixed at 120 V, rather hysteresis is kept around upper and lower cut off limits i.e 'V^{G}_{max}'=122.5 and 'V^{G}_{min}'=117.5 V respectively. Therefore, a balanced load and bidirectional flow of power is maintained throughout the operation to ensure the stability of grid.

Fig. 10. DGDSA Microgrid Hardware Implementation from the integrations of Nanogrids. House 1 is Modeled using Power Supply and continuously supplying power. House 2 is Modeled using 4-quardant power supply and can supply as well as demand power. House 3 is modeled by a battery along with bi-directional flyback converter interfaced with house 1 and house 2 through grid which is modeled as capacitor

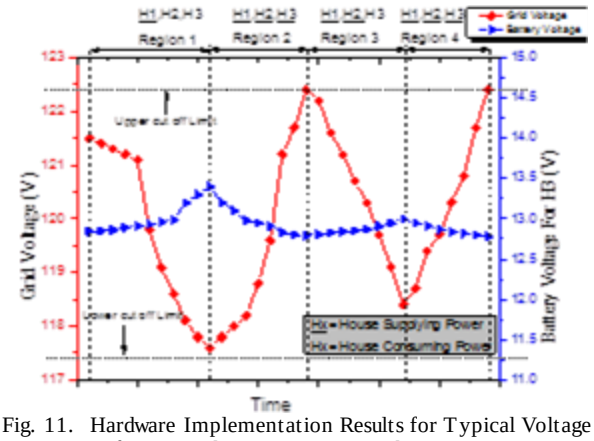

Fig. 11. Hardware Implementation Results for Typical Voltage Variations of Microgrid in Various Power Sharing Scenarios

VIII. CONCLUSION

This work presents a novel and efficient DC microgrid architecture for rural electrification with emphasis on beyond subsistence level power provision. Results show that the proposed distributed generation distributed storage architecture can have approximately 5% higher distribution efficiency compared to other LVDC architectures. Moreover, the proposed DGDSA is scalable in terms of its design and operation. These gains in terms of efficiency and scalability are achieved through a modular interconnection of various contributing households (nanogrids) with distributed control through hysteretic voltage droop method. This distributed solar PV generation as well as storage allows power sharing viable for driving larger communal loads not available in any other existing architecture. For a typical village arrangement in a developing region with 40 households, distribution efficiency of 96% can be achieved for a typical 2.5 mm^2 conductor even at low distribution voltage of 120V DC (ring-main topology) with peak load sharing capability. The proposed architecture is therefore ideal for, beyond subsistence level, rural electrification in developing countries.

REFERENCES

[1] R. Singh and K. Shenai, "DC microgrids and the virtues of local electricity," *IEEE Spectrum*, 2014.

[2] P. Brinckerhoff, "Electricity Transmission Costing Study: An independent report endorsed by the Institute of Engineering & Technology," ed: London, 2012.

[3] "World energy outlook 2015," *International Energy Agency*, vol. 1, 2015.

[4] M. N. Qaiser, M. Usama, B. Ahmad, M. A. Tariq, and H. A. Khan, "Low Cost, Robust and Efficient Implementation of MPPT based Buck-Boost Converter for Off-grid PV Applications," presented at the 40th IEEE Photovoltaic Specialists Conference, Denver Colorado, USA, 2014.

[5] H. A. Khan and S. Pervaiz, "Technological review on solar PV in Pakistan: Scope, practices and recommendations for optimized system design," *Renewable and Sustainable Energy Reviews*, vol. 23, pp. 147-154, 2013.

[6] S. H. I. Jaffery, M. Khan, L. Ali, H. A. Khan, R. A. Mufti, A. Khan, N. Khan, and S. M. Jaffery, "The potential of solar powered transportation and the case for solar powered railway in Pakistan," *Renewable and Sustainable Energy Reviews*, vol. 39, pp. 270-276, 2014.

[7] J. Khan and M. H. Arsalan, "Solar power technologies for sustainable electricity generation–A review," *Renewable and Sustainable Energy Reviews*, vol. 55, pp. 414-425, 2016.

[8] P. A. Madduri, J. Rosa, S. R. Sanders, E. A. Brewer, and M. Podolsky, "Design and verification of smart and scalable DC microgrids for emerging regions," in *Energy Conversion Congress and Exposition (ECCE), 2013 IEEE*, 2013, pp. 73-79.

[9] D. Soto and V. Modi, "Simulations of Efficiency Improvements Using Measured Microgrid Data," in *Global Humanitarian Technology Conference (GHTC), 2012 IEEE*, 2012, pp. 369-374.

[10] J. J. Justo, F. Mwasilu, J. Lee, and J.-W. Jung, "AC-microgrids versus DC-microgrids with distributed energy resources: A review," *Renewable and Sustainable Energy Reviews*, vol. 24, pp. 387-405, 2013.

[11] V. M. Balijepalli, S. Khaparde, and C. Dobariya, "Deployment of microgrids in India," in *IEEE PES General Meeting*, 2010, pp. 1-7.

[12] P. Loomba, S. Asgotraa, and R. Podmore, "DC solar microgrids—A successful technology for rural sustainable development," in *PowerAfrica, 2016 IEEE PES*, 2016, pp. 204-208.

[13] D. Palit, G. K. Sarangi, and P. Krithika, "Energising Rural India Using Distributed Generation: The Case of Solar Mini-Grids in Chhattisgarh State, India," in *Mini-Grids for Rural Electrification of Developing Countries*, ed: Springer, 2014, pp. 313-342.

[14] D. Palit and G. K. Sarangi, "Renewable energy based mini-grids for enhancing electricity access: Experiences and lessons from India," in *International Conference and Utility Exhibition on Green Energy for Sustainable Development (ICUE)*,\ 19-21 March 2014, pp. 1-8.

[15] P. A. Madduri, J. Poon, J. Rosa, M. Podolsky, E. Brewer, and S. R. Sanders, "Scalable DC Microgrids for Rural Electrification in Emerging Regions," *IEEE Journal of Emerging and Selected Topics in Power Electronics*, vol. PP, pp. 1-1, 2016.

[16] M. Nasir, N. A. Zaffar, and H. A. Khan, "Analysis on central and distributed architectures of solar powered DC microgrids," in *2016 Clemson University Power Systems Conference (PSC)*, 2016, pp. 1-6.

[17] F. Pearce. World's poor need grid power, not just solar panels. *Energy and Fuels 2980, 2014*.

[18] W. Inam, D. Strawser, K. K. Afridi, R. J. Ram, and D. J. Perreault, "Architecture and system analysis of microgrids with peer-to-peer electricity sharing to create a marketplace which enables energy access," in *Power Electronics and ECCE Asia (ICPE-ECCE Asia), 2015 9th International Conference on*, 2015, pp. 464-469.

[19] J. Chi, W. Peng, X. Jianfang, T. Yi, and C. Fook Hoong, "Implementation of Hierarchical Control in DC Microgrids," *Industrial Electronics, IEEE Transactions on*, vol. 61, pp. 4032-4042, 2014.

[20] T. Vandoorn, J. De Kooning, B. Meersman, and L. Vandevelde, "Review of primary control strategies for islanded microgrids with power-electronic interfaces," *Renewable and Sustainable Energy Reviews*, vol. 19, pp. 613-628, 2013.

[21] T. Dragičević, J. M. Guerrero, J. C. Vasquez, and D. Škrlec, "Supervisory control of an adaptive-droop regulated DC microgrid with battery management capability," *IEEE Transactions on Power Electronics*, vol. 29, pp. 695-706, 2014.

[22] C. S. Solanki, *Solar photovoltaics: fundamentals, technologies and applications*: PHI Learning Pvt. Ltd., 2011.

[23] B. Subudhi and R. Pradhan, "A comparative study on maximum power point tracking techniques for photovoltaic power systems," *Sustainable Energy, IEEE transactions on*, vol. 4, pp. 89-98, 2013.

[24] M. Nasir and M. F. Zia, "Global maximum power point tracking algorithm for photovoltaic systems under partial shading conditions," in *Power Electronics and Motion Control Conference and Exposition (PEMC), 2014 16th International*, 2014, pp. 667-672.

[25] R. Pasonen, "Model of Bi-directional Flyback Converter for Hybrid AC/DC Distribution System," *International Journal of Power Electronics and Drive Systems (IJPEDS)*, vol. 3, pp. 444-449, 2013.

[26] V. Mehta and R. Mehta, *Principles of power system*: S. Chand, 1982.

[27] H. Saadat, *Power system analysis*: WCB/McGraw-Hill, 1999.

[28] K. R. Varshney, G. H. Chen, B. Abelson, K. Nowocin, V. Sakhrani, L. Xu, and B. L. Spatocco, "Targeting villages for rural development using satellite image analysis," *Big Data*, vol. 3, pp. 41-53, 2015.

[29] I. Marx, "Combining the best of both worlds," *Industry Applications Magazine, IEEE*, vol. 16, pp. 30-34, 2010.

[30] A. F. X. Welsch, "DC Installation, Different Hazards Regarding Thermal Effects and Electrical Shock," *IEC LVDC Workshop, University of Applied Science, Regensburg*, 2011.

[31] LABTECH (LEMSPL) [Online]. Available: http://www.eepowersolutions.com/products/portable-dc-load-banks-with-monitoring/

[32] EPS- 6030T [Online]. Available: http://www.wavecom.com.au/04_product_documents/688/Brochure_EPS_6030T%20Power%20Supply_Ver_0.pdf

[33] KEPCO BOP 2001-D KEPCO, Inc. [Online]. Available: http://www.kepcopower.com/bop.htm